SRC-TR-87-47

Steady State Behavior of A Continuous Stirred Tank Reactor for Styrene Polymerization with Bifunctional Free Radical Initiators

by

K.J. Kim
K.Y. Choi

Steady State Behavior of A Continuous Stirred Tank Reactor for Styrene Polymerization with Bifunctional Free Radical Initiators

by

K. J. Kim and K. Y. Choi*

Department of Chemical and Nuclear Engineering
and Systems Research Center
University of Maryland
College Park, MD 20742

Submitted to: Chem. Eng. Sci. (1987)

* To whom correspondence should be addressed

Abstract

Steady state behavior of a continuous stirred tank reactor is analyzed for styrene polymerization with bifunctional free radical initiators. Compared with polymerization by monofunctional initiators, the bifunctional initiator system produces polymers of significantly high molecular weight at high monomer conversion. This is due to the presence of multiple labile peroxide groups having distinctively different thermal decomposition characteristics. The steady state reactor model analysis indicates that five unique regions of steady state behavior are present in a parameter space with reactor residence time as a bifurcation parameter. It is also shown that a broad range of polymer properties can be obtained by judiciously choosing the reactor operating conditions with the bifunctional initiator.

Introduction

Over the past few years, many papers have been published on the modeling and control of free radical polymerization reactors. The thrust of current research resides in the development of advanced polymerization technology through improved understanding of the polymerization kinetics and reactor behavior, and implementation of sophisticated reactor control algorithms in order to tailor polymer properties. In many industrial polymerization processes a variety of initiator systems are practiced to produce polymers of various grades to meet diversified enduse requirements. It is quite surprising, however, that in most of the works reported in the literature only simple monofunctional initiators such as benzoyl peroxide or azobisisobutyronitrile (AIBN) have been considered.

Multifunctional initiators are the initiators which contain more than one labile group (e.g. peroxy, perester, azo groups) having distinctively different thermal decomposition characteristics. Although the idea of using multifunctional initiators in free radical polymerization was introduced many years ago, it is only recently that systematic quantitative studies of polymerization kinetics with such multifunctional initiator systems have been performed (O'Driscoll and Bevington, 1985; Choi and Lei, 1986). Moreover, there is a rapidly growing industrial interest in using the multifunctional initiators to produce reactive polymers and polymers of precisely tuned properties more economically. By using properly chosen multifunctional initiators, one can achieve both high monomer conversion and significantly high polymer molecular weight simultaneously. Some multifunctional initiators have also been used for block copolymerization of vinyl monomers via controlled sequential monomer incorporation technique (Piirma and Chou, 1979; Gunesin and Piirma, 1981; Waltz and Heitz,1978). One of the main attraction of multifunctional initiators is that no major modification of existing polymerization equipment is required and implementation of them into the polymerization processes can be made easily. The use of multifunctional initiators also offers added flexibilities to polymer reactor engineers in optimizing polymerization reactor performance. However, the polymerization kinetics with multifunctional initiators are quite complex and understanding the polymerization characteristics is essential in applying the multifunctional initiators to industrial polymerization processes employing various reactor configurations.

In this paper, we shall present a detailed analysis of steady state behavior of a continuous stirred tank reactor for styrene polymerization with bifunctional initiator system which is of the simplest form of the multifunctional initiators. In particular, the effect of bifunctional initiators on the polymer molecular weight properties will be elucidated.

Polymerization Kinetics

The bifunctional initiator system to be considered in this study is the diperoxyesters of the following structurally symmetrical form:

$$R_1COO-OOCXCOO-OOCR_1 \tag{1}$$

where R_1 and X represent hydrocarbon ligands. The specific initiator system chosen in our numerical simulation study is the diperoxyester studied by Prisyazhnyuk and Ivanchev (1970):

$$\underset{(I)}{CH_3(CH_2)_6COO-OOCCH_2CHClCOO-OOC(CH_2)_6CH_3} \tag{2}$$

Upon heating, the initiator decomposes into two radical species as follows:

$$I \xrightarrow{\Delta} \underset{(R)}{CH_3(CH_2)_6COO\cdot} + \cdot \underset{(R')}{OOCCH_2CHClCOO-OOC(CH_2)_6CH_3} \tag{3}$$

where the primary radical species R' carries an undecomposed peroxide group which may decompose further during the course of polymerization. The above authors found that the decomposition activation energy of the peroxide group in R' is quite different from that of the peroxides in the original initiator (I). This characteristic is generally true for many other structurally symmetrical diperoxide initiators (Ivanchev, 1979). When monomers are polymerized by the radical species R', the polymers will carry labile peroxide groups and such polymers are called reactive polymers or polymeric initiators. As will be shown in what follows, quite complex reinitiation, propagation and termination reaction kinetics are resulted due to the existence of the two radical species (R and R') in the polymerization reactor.

A mechanism of polymer formation in free radical polymerization initiated by bifunctional initiators is called poly-recombinational polymerization because reactive macromolecules formed in the early stages of polymerization participate in the reaction through re-initiation, propagation and termination. As shown in Table 1, six different polymeric species (P_n, Q_n, S_n, T_n, Z_n, and M_n) can be defined in accordance with the nature of the end units of the polymer chains. Note that P_n, Q_n, and S_n are the growing (or live) polymer radicals with n-monomer units and T_n, Z_n, and M_n are the dead polymers of n-monomer units. However, Q_n, T_n, and Z_n species carry undecomposed peroxide groups (–COO–OOCR$_1$) on the chain ends. Thus, such polymers can be reconverted to active radical species via subsequent thermal decomposition of the peroxides. The decomposition reactions of the primary diperoxyester initiator (I) and the polymeric initiators can be described as following:

$$I \xrightarrow{k_{d_1}} R + R' \tag{4}$$

$$Q_1 \xrightarrow{k_{d_2}} S_1 + R \tag{5.a}$$

$$Q_n \xrightarrow{k_{d_2}} S_n + R \qquad (n \geq 2) \tag{5.b}$$

$$T_n \xrightarrow{k_{d_2}} Q_n + R \qquad (n \geq 2) \tag{6}$$

$$Z_n \xrightarrow{k_{d_2}} P_n + R \qquad (n \geq 2) \tag{7}$$

where k_{d1} and k_{d2} denote the decomposition rate constants of the two peroxide groups in the primary initiators and in the polymers, respectively. Here, it is assumed that cyclization reaction and thermal initiation do not occur. The decomposition of primary radical species R' is also assumed negligible. According to Ivanchev (1977), the decomposition rate constants of more stable peroxides (i.e., peroxides in Q_n, T_n and Z_n) are independent of polymer chain length.

Table 1. Polymeric species

Growing Polymers

P_n : $\cdot$ ———— $OOCR_1$

Q_n : $\cdot$ ———— $COO-OOCR_1$

S_n : $\cdot$ ———— $\cdot$

Inactive Polymers

T_n : $R_1COO-OOC$ ———— $COO-OOCR_1$

Z_n : R_1COO ———— $COO-OOCR_1$

M_n : R_1COO ———— $OOCR_1$

The initiation of polymer chain propagation by the primary radicals takes place as follows:

$$R + M \xrightarrow{k_{i_1}} P_1 \tag{8}$$

$$R' + M \xrightarrow{k_{i_2}} Q_1 \tag{9}$$

The propagation reactions are:

$$P_1 + M \xrightarrow{k_p} P_2 \tag{10.a}$$

$$P_n + M \xrightarrow{k_p} P_{n+1} \qquad (n \geq 2) \tag{10.b}$$

$$Q_1 + M \xrightarrow{k_p} Q_2 \tag{11.a}$$

$$Q_n + M \xrightarrow{k_p} Q_{n+1} \qquad (n \geq 2) \tag{11.b}$$

$$S_1 + M \xrightarrow{k_p} S_2 \tag{12.a}$$

$$S_n + M \xrightarrow{k_p} S_{n+1} \qquad (n \geq 2) \tag{12.b}$$

where the propagation rate constants are also assumed to be independent of polymer chain length. When the termination of growing polymer chains occurs exclusively by combination mechanism (e.g. styrene polymerization), the following termination reactions will take place:

$$P_n + P_m \xrightarrow{k_t} M_{n+m} \qquad (n, m \geq 1) \tag{13}$$

$$P_n + Q_m \xrightarrow{k_t} Z_{n+m} \qquad (n, m \geq 1) \tag{14}$$

$$P_n + S_m \xrightarrow{k_t} P_{n+m} \qquad (n, m \geq 1) \tag{15}$$

$$Q_n + Q_m \xrightarrow{k_t} T_{n+m} \qquad (n, m \geq 1) \tag{16}$$

$$Q_n + S_m \xrightarrow{k_t} Q_{n+m} \qquad (n, m \geq 1) \tag{17}$$

$$S_n + S_m \xrightarrow{k_t} S_{n+m} \qquad (n, m \geq 1) \tag{18}$$

Note that various reactive polymeric species (e.g. Q_n, T_n, Z_n) containing undecomposed peroxide groups are formed by the combination termination reactions and these species, upon subsequent decomposition and polymerization, will lead to the formation of polymers having extended polymer chain lengths. The termination by primary radicals is assumed negligible in the above scheme. In Eqs. (13)~(18), the combination termination rate constants for the different polymeric species are assumed to be identical. In this kinetic scheme, chain transfer reactions have been ignored.

With the polymerization mechanism proposed above, batch polymerization kinetics with the bifunctional initiator can be modeled as follows:

For Initiator and Primary Radicals

$$\frac{dI}{dt} = -k_{d_1} I \tag{19}$$

$$\frac{dR}{dt} = f_1 k_{d_1} I - k_{i_1} RM + k_{d_2}(Q + T + Z) \tag{20}$$

$$\frac{dR'}{dt} = f_2 k_{d_1} I - k_{i_2} R'M \tag{21}$$

where f_1 and f_2 are the initiator efficiencies which indicate the fraction of primary radicals (R and R') being involved in chain initiation.

For Growing Polymers

$$\frac{dP_1}{dt} = k_{i_1} RM - k_p M P_1 - k_t P_1 (P + Q + S) \tag{22}$$

$$\frac{dP_n}{dt} = k_p M (P_{n-1} - P_n) + k_{d_2} Z_n - k_t P_n (P + Q + S) + k_t \sum_{m=1}^{n-1} P_{n-m} S_m \qquad (n \geq 2) \tag{23}$$

$$\frac{dQ_1}{dt} = k_{i_2} R' M - k_p M Q_1 - k_{d_2} Q_1 - k_t Q_1 (P + Q + S) \tag{24}$$

$$\frac{dQ_n}{dt} = -k_{d_2} Q_n + k_{d_2} T_n + k_p M (Q_{n-1} - Q_n) - k_t Q_n (P + Q + S) + k_t \sum_{m=1}^{n-1} Q_{n-m} S_m \qquad (n \geq 2) \tag{25}$$

$$\frac{dS_1}{dt} = k_{d_2} Q_1 - k_p M S_1 - k_t S_1 (P + Q + S) \tag{26}$$

$$\frac{dS_n}{dt} = k_{d_2} Q_n + k_p M (S_{n-1} - S_n) - k_t S_n (P + Q + S) + \frac{k_t}{2} \sum_{m=1}^{n-1} S_{n-m} S_m \qquad (n \geq 2) \tag{27}$$

For Temporarily Inactive Polymers

$$\frac{dT_n}{dt} = -k_{d_2} T_n + \frac{k_t}{2} \sum_{m=1}^{n-1} Q_{n-m} Q_m \qquad (n \geq 2) \tag{28}$$

$$\frac{dZ_n}{dt} = -k_{d_2} Z_n + k_t \sum_{m=1}^{n-1} P_{n-m} Q_m \qquad (n \geq 2) \tag{29}$$

For Monomers and Dead Polymers

$$\frac{dM}{dt} = -k_{i_1} RM - k_{i_2} R'M - k_p M(P+Q+S) \tag{30}$$

$$\frac{dM_n}{dt} = \frac{k_t}{2} \sum_{m=1}^{n-1} P_{n-m} P_m \qquad (n \geq 2) \tag{31}$$

where P, Q, S, T, and Z are the total concentrations of the corresponding polymeric species, i.e.,

$$\begin{aligned} P &= \sum_{n=1}^{\infty} P_n \qquad Q = \sum_{n=1}^{\infty} Q_n \qquad S = \sum_{n=1}^{\infty} S_n \\ T &= \sum_{n=2}^{\infty} T_n \qquad Z = \sum_{n=2}^{\infty} Z_n \end{aligned} \tag{32}$$

For primary radicals and live polymeric species (P_n, Q_n, and S_n) quasi-steady state approximation will be employed. In order to compute the molecular weight averages of polymers, the following molecular weight moments are used:

$$\lambda_{\xi,k} \equiv \sum_{n=j}^{\infty} n^k \xi_n \qquad \left(\xi = P, Q, S(j=1); T, Z(j=2)\right) \tag{33}$$

$$\lambda_k^d \equiv \sum_{n=2}^{\infty} n^k M_n \tag{34}$$

where $\lambda_{\xi,k}$ and λ_k^d denote the k-th moment of polymeric species ξ and dead polymers, respectively.

In high conversion free radical polymerization, the termination reactions involving polymeric radicals become diffusion controlled and the termination rate constant decreases considerably with conversion. This phenomenon is referred to as gel-effect. Although the gel effect in styrene polymerization is not as strong as in methyl methacrylate polymerization, the gel effect is not quite negligible at high conversion or low solvent volume fraction. In this study, the gel effect correlation suggested by Friis and Hamielec (1976) for bulk styrene polymerization is used and modified for solution polymerization according to Hamer et al. (1981):

$$g_t \equiv \frac{k_t}{k_{to}} = exp\left[-2(BX + CX^2 + DX^3)\right] \tag{35}$$

where

$$B = 2.57 - 5.05 \times 10^{-3}T \ \ (^\circ\mathrm{K})$$

$$C = 9.56 - 1.76 \times 10^{-2}T \ \ (^\circ\mathrm{K})$$

$$D = -3.03 + 7.85 \times 10^{-3}T \ \ (^\circ\mathrm{K})$$

and

$$X = X_1(1 - f_s)$$

is the total concentration of monomer in the presence of solvent with volume fraction of f_s. k_{to} denotes the termination rate constant at zero monomer conversion. Figure 1 illustrates the variation in chain termination rate constants predicted by Eq. (35) for different temperatures and solvent fractions, respectively. The incorporation of the gel effect correlation into the model improves the model accuracy and increases the model complexity as well.

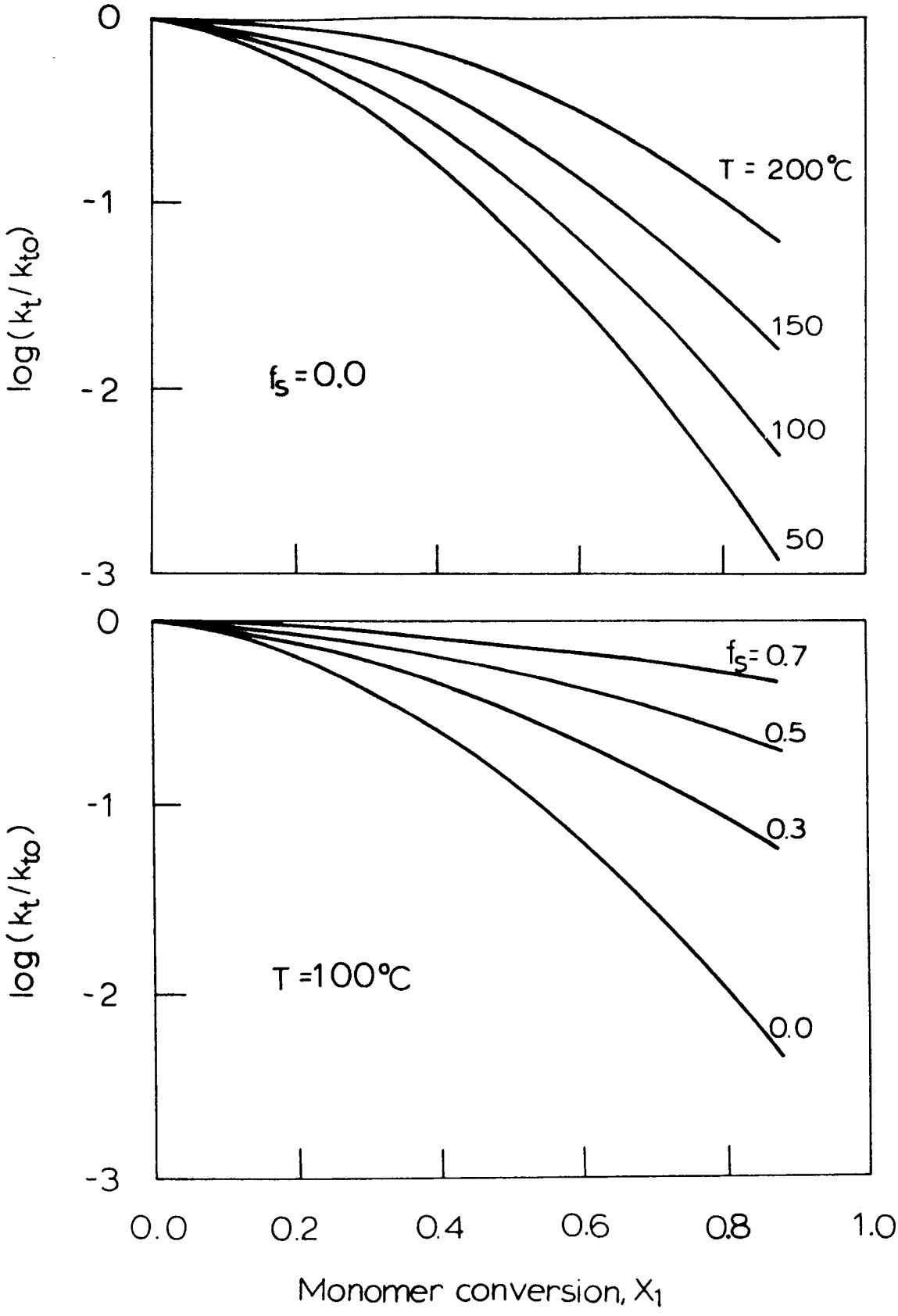

Figure 1 Gel effect correlations for styrene polymerization

Ractor Model

For free radical homopolymerization of styrene with bifunctional initiator in a continuous stirred tank reactor of volume V, mass and energy balances are represented by the following equations:

$$V\frac{dM}{dt'} = q(M_f - M) - Vk_pM(P+Q+S) \tag{36}$$

$$V\frac{dI}{dt'} = q(I_f - I) - Vk_{d1}I \tag{37}$$

$$\begin{aligned}\rho C_pV\frac{dT}{dt'} = {} & \rho C_pq(T_f - T) + V(-\Delta H_r)k_pM(P+Q+S) \\ & - h_cA_c(T - T_c)\end{aligned} \tag{38}$$

Here, M is the monomer concentration, I the initiator concentration, and T the reactor temperature. q denotes the volumetric flow rate of feed and product streams, h_c the effective heat transfer coefficient and T_c the coolant temperature. Physical properties of the polymer mixture (e.g. ρ, C_p) are assumed constant. In this model, the effects of thermal initiation and depolymerization which may occur at very high temperatures are ignored. Due to the presence of active polymeric species (P_n, Q_n, S_n) and inactive polymeric species (T_n, Z_n, M_n), the above nonlinear modeling equations become quite complicated.

The moment equations for inactive polymers (species M_n, T_n and Z_n) take the following form:

$$\frac{d\lambda_0^d}{dt'} = -\frac{1}{\theta}\lambda_0^d + \frac{1}{2}k_t\lambda_{P,0}^2 \tag{39.a}$$

$$\frac{d\lambda_1^d}{dt'} = -\frac{1}{\theta}\lambda_1^d + k_t\lambda_{P,0}\lambda_{P,1} \tag{39.b}$$

$$\frac{d\lambda_2^d}{dt'} = -\frac{1}{\theta}\lambda_2^d + k_t(\lambda_{P,0}\lambda_{P,2} + \lambda_{P,1}^2) \tag{39.c}$$

$$\frac{d\lambda_{T,0}}{dt'} = -\frac{1}{\theta}\lambda_{T,0} + \frac{1}{2}k_t\lambda_{Q,0}^2 - k_{d2}\lambda_{T,0} \tag{40.a}$$

$$\frac{d\lambda_{T,1}}{dt'} = -\frac{1}{\theta}\lambda_{T,1} + k_t\lambda_{Q,0}\lambda_{Q,1} - k_{d2}\lambda_{T,1} \tag{40.b}$$

$$\frac{d\lambda_{T,2}}{dt'} = -\frac{1}{\theta}\lambda_{T,2} + k_t(\lambda_{Q,0}\lambda_{Q,2} + \lambda_{Q,1}^2) - k_{d2}\lambda_{T,2} \tag{40.c}$$

$$\frac{d\lambda_{Z,0}}{dt'} = -\frac{1}{\theta}\lambda_{Z,0} + k_t\lambda_{P,0}\lambda_{Q,0} - k_{d2}\lambda_{Z,0} \tag{41.a}$$

$$\frac{d\lambda_{Z,1}}{dt'} = -\frac{1}{\theta}\lambda_{Z,1} + k_t(\lambda_{P,0}\lambda_{Q,1} + \lambda_{P,1}\lambda_{Q,0}) - k_{d2}\lambda_{Z,1} \tag{41.b}$$

$$\frac{d\lambda_{Z,2}}{dt'} = -\frac{1}{\theta}\lambda_{Z,2} + k_t(\lambda_{P,0}\lambda_{Q,2} + 2\lambda_{P,1}\lambda_{Q,1} + \lambda_{P,2}\lambda_{Q,0}) - k_{d2}\lambda_{Z,2} \tag{41.c}$$

The number average polymer chain length (X_N) and the weight average chain length (X_W) are defined by

$$X_N = \frac{\lambda_{P,1} + \lambda_{Q,1} + \lambda_{S,1} + \lambda_{T,1} + \lambda_{Z,1} + \lambda_1^d}{\lambda_{P,0} + \lambda_{Q,0} + \lambda_{S,0} + \lambda_{T,0} + \lambda_{Z,0} + \lambda_0^d} \tag{42.a}$$

$$X_W = \frac{\lambda_{P,2} + \lambda_{Q,2} + \lambda_{S,2} + \lambda_{T,2} + \lambda_{Z,2} + \lambda_2^d}{\lambda_{P,1} + \lambda_{Q,1} + \lambda_{S,1} + \lambda_{T,1} + \lambda_{Z,1} + \lambda_1^d} \tag{42.b}$$

where $\lambda_{j,k}$ represents the k-th moment of polymeric species j. The polydispersity index (PD) is a measure of molecular weight distribution broadening and is defined by

$$PD = \frac{X_W}{X_N} \tag{43}$$

The moment equations (39)~(41) are solved simultaneously with reactor modeling equations.

Steady State Model Analysis

The modeling equations are reduced to dimensionless forms by using the following dimensionless variables and parameters:

$$
\begin{aligned}
&X_1 = \frac{M_f - M}{M_f}, \qquad X_2 = \frac{I_f - I}{I_f}, \qquad X_3 = \frac{T - T_f}{T_f}, \\
&X_p = \frac{P+Q+S}{P_f+Q_f+S_f}, \qquad \alpha = \frac{h_c A_c}{\rho C_p V \kappa(T_f)}, \qquad \beta = \frac{(-\Delta H_r)M_f}{\rho C_p T_f}, \\
&\gamma = \frac{E_p}{RT_f}, \qquad \gamma_1 = \frac{E_{d1}}{RT_f}, \qquad \delta = \frac{T_c - T}{T_f}, \\
&Da = \theta\kappa(T_f), \qquad t = \frac{t'}{\theta}, \qquad K = \frac{k_{d10}}{\kappa(T_f)}
\end{aligned}
\tag{44}
$$

where

$$\kappa(T_f) = k_{p0}(P+Q+S)_f \exp\left(\frac{E_p}{RT_f}\right)$$

The subscript f denotes the feed condition. Then, the following dimensionless modeling equations are obtained:

$$\frac{dX_1}{dt} = -X_1 + Da(1-X_1)X_p \exp\left[\frac{\gamma X_3}{1+X_3}\right] \tag{45}$$

$$\frac{dX_2}{dt} = -X_2 + KDa(1-X_2)\exp\left[-\frac{\gamma_1}{1+X_3}\right] \tag{46}$$

$$\frac{dX_3}{dt} = -X_3 + \beta\left(X_1 + \frac{dX_1}{dt}\right) - \alpha Da(X_3 - \delta) \tag{47}$$

Note that α refers to the dimensionless heat transfer coefficient, β the dimensionless heat of reaction, and Da the dimensionless mean residence time which can be changed experimentally by varing the reactant flow rate. Because of high degree of nonlinearity and interaction in the modeling equations, some care must be taken in obtaining the steady state solutions. At steady state, the LHS of the modeling equations (45)~(47) vanish and the steady state solutions are computed by the following procedure.

(i) For fixed value of Da, use Eqs. (46) and (47) to obtain:

$$X_{2s} = \frac{KDa\exp[-\frac{\gamma_1}{1+X_{3s}}]}{1+KDa\exp[-\frac{\gamma_1}{1+X_{3s}}]} \tag{48}$$

$$X_{3s} = \frac{\beta X_{1s} + \alpha Da\delta}{1+\alpha Da} \tag{49}$$

where subscript s denotes the steady state condition.

(ii) Substitute Eqs. (48) and (49) to Eq. (45) and solve the resulting nonlinear equation for monomer conversion X_1, $(0 \leq X_1 \leq 1)$. The dimensionless total live polymer concentration (X_p) is computed by solving the following equations which are from the steady state zeroth momont equations of P, Q and S:

$$a_1 - a_2(P+Q)P + a_3Q + a_4(\frac{1}{2}Q^2 + 2PQ) = 0 \tag{50}$$

$$Q = \frac{1}{2(a_2 - a_4/2)}[-a_2P - a_3 + \{(a_2P+a_3)^2 + 4a_1(a_2 - \frac{a_4}{2})\}^{\frac{1}{2}}] \tag{51}$$

$$S = -(P+Q) + [(P+Q)^2 + 2(\frac{a_3}{a_2})Q]^{\frac{1}{2}} \tag{52}$$

where

$$a_1 = f_i k_{d10} I_f (1-X_2)\exp[-\frac{\gamma_1}{1+X_3}],$$

$$a_2 = k_{t0} g_t \exp[-\frac{\gamma_t}{1+X_3}], \qquad a_3 = k_{d20}\exp[-\frac{\gamma_d}{1+X_3}],$$

$$a_4 = \frac{a_2 a_3 \theta}{1+a_3\theta}, \qquad \gamma_t = \frac{E_t}{RT_f}, \qquad \gamma_d = \frac{E_{d2}}{RT_f}.$$

(iii) Vary Da and repeat steps (i) and (ii).

This procedure guarantees that all solutions are found for all admissible values of Da. The mathematical expressions of steady state polymer moments are given in Appendix. The numerical values of physical constants, kinetic parameters and standard reactor operating conditions are listed in Table 2. Note that the monofunctional initiators (A1 and A2) are hypothetical ones used for the purpose of comparison with the bifunctional initiator system. The behavior of the monofunctional initiator A2 is similiar to that of popular azobisisobutyronitrile (AIBN).

Results and Discussion

The principal parameters which influence the behavior of the continuous styrene solution polymerization reactors are Da (or θ), α, β (or f_s), γ, γ_1 and δ. For given values of the system parameters the steady states may be calculated by solving the steady state nonlinear equations (45)~(47). In practical situations, one is often interested in knowing the steady state multiplicity pattern existing for a given set of system parameters. With parameters δ, T_f and I_f held fixed, the diagram showing the steady state behavior of the reactor has been constructed by using the method developed by Balakotaiah and Luss (1981). Figure 2 is a such diagram in α-β plane for the bifunctional initiator system. Note that five unique regions of steady state behavior are identified:

Region I :	Unique steady state
Region II :	Multiple steady state (S-shape curve)
Region III:	Isola and unique steady state
Region IV:	Isola and multiple steady state (S-shape curve)
Region V :	Mushroom

Here, Γ_1 (Γ_2) represents the hysteresis (isola) variety which defines the parameter space at which a continuous change of the parameter causes the appearance or disappearance of hysteresis (isola) type multiplicity (Balakotaiah and Luss, 1981).

Table 2. Numerical values of kinetic parameters and standard operating conditions for styrene polymerization

	Ref*
k_{d1}=6.824 × 10^{10}exp(-22,800/RT), sec^{-1}	[1]
k_{d2}=6.594 × 10^{14}exp(-30,500/RT), sec^{-1}	[1]
k_p=1.051 × 10^7exp(-7,060/RT), l/mol.sec	[2]
k_t=1.255 × 10^9exp(-1,680/RT), l/mol.sec	[2]
f_i=0.23 (i = 1, 2)	[1]
$(-\Delta H_r)$=16.2 Kcal/mol	[2]
ρC_p=0.4 Kcal/l°K	[2]

For Monofunctional Initiators:

(A1) k_d=6.824 × 10^{10}exp(-22,800/RT), sec^{-1}
f_i=0.23

(A2) k_d=6.594 × 10^{14}exp(-30,500/RT), sec−1
f_i=0.23

T_f=300 °K, T_c=303 °K, I_f=0.05 mol/l
f_s=0.0∼1.0, α=0∼100

* [1] Prinsyahnyuk and Ivanchev (1970)
[2] Brandrup and Immergut (1975)

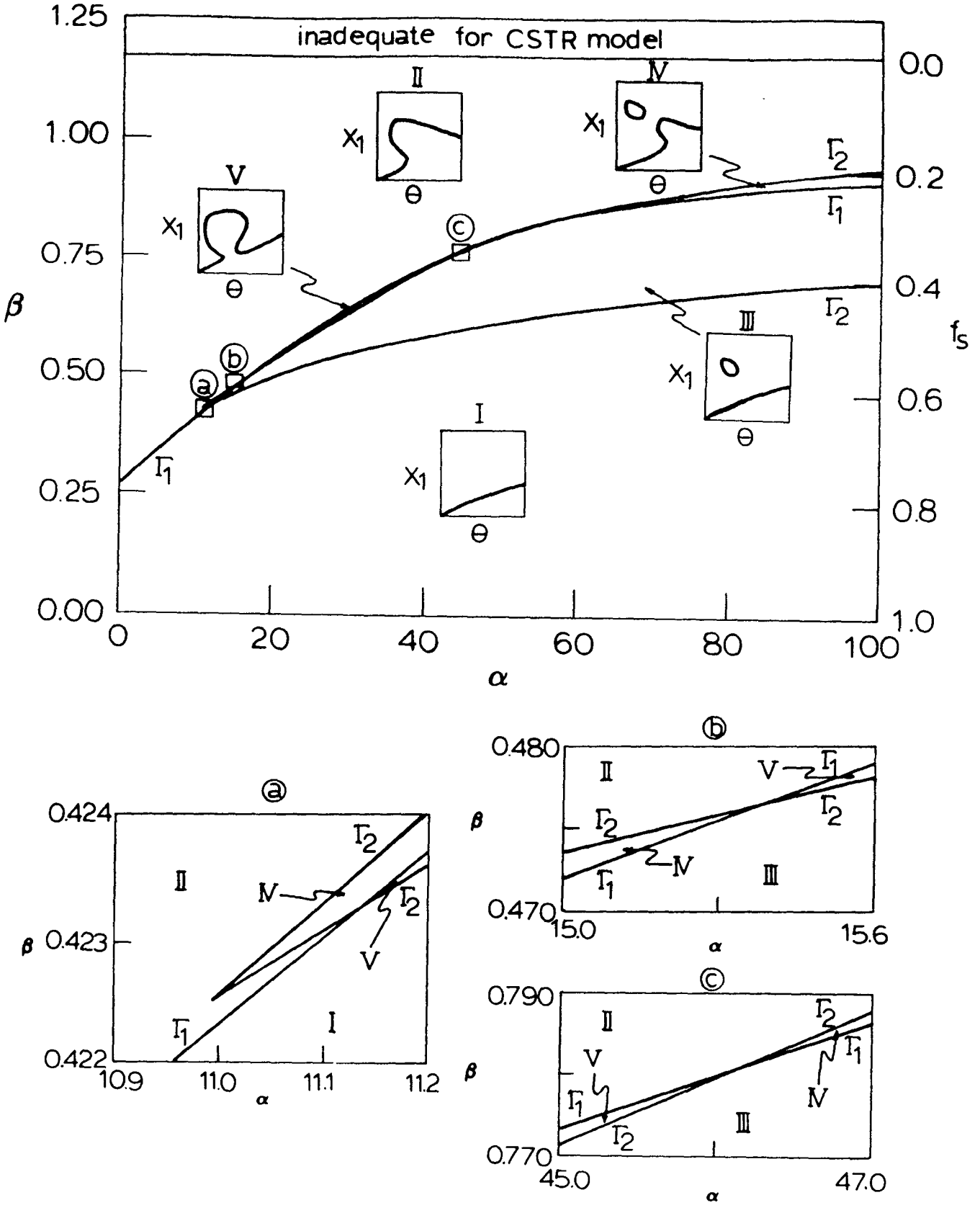

Figure 2 Steady state behavior regions for styrene polymerization in a CSTR with bifunctinal initiator, δ=0.01, I_{fB}=0.025 mol/l.

Here, the criteria for the hysteresis variety (i.e., the appearance of multiple steady state) are:

$$F(X_1, Da, \beta) = 0 \tag{53.a}$$

$$\frac{\partial F}{\partial X_1}(X_1, Da, \beta) = 0 \tag{53.b}$$

$$\frac{\partial^2 F}{\partial^2 X_1}(X_1, Da, \beta) = 0 \tag{53.c}$$

in which F represents a steady state manifold obtained by combining three modeling equations (45)~(47) into one by eliminating X_2 and X_3 for fixed value of α. Across the hysteresis variety the number of solutions increases by 2 for increasing value of α. The criteria for the isola variety are given by Eqs. (53.a), (53.b) and:

$$\frac{\partial F}{\partial Da}(X_1, Da, \beta) = 0 \tag{53.d}$$

For a sequence of α, Eqs. (53.a)~(53.c) for the hysteresis variety and Eqs. (53.a),(53.b) and (53.d) for the isola variety have been solved by using the Brown's method (Computational details can be found in Kim, 1989). In regions III and IV, isolated branches (isola) are observed. The existence of isola phenomena has been known for many years in various chemically reacting systems including continuous polymerization reactors (Schmidt et al., 1984). The isola cannot be obtained by simply varying the reactor residence time and special control scheme is required to operate the reactor at such steady state conditions. Since regions IV and V are so small, it will be practically very difficult to confirm these tiny regions experimentally. This means that most of the reactor behavior will be represented by region I, II and III for practical operating conditions. It is also interesting to observe that unique steady state behavior is never expected in bulk free radical polymerization reactors (i.e., $f_s = 0.0$). For adiabatic polymerization (i.e., $\alpha = 0.0$), only type I and II

steady state profiles will appear. Figures 3(a) and 3(b) show the similar steady state behavior diagrams for the monofunctional initiator systems A1 and A2, respectively. The overall structures of the steady state behavior regions for the bifunctional initiator system and for the monofunctional initiator systems are quite similar. The concentration of peroxide groups in the initiator feed stream is held fixed at the same value for all cases, i.e., $I_{fB} = \frac{1}{2} I_{fA1} = \frac{1}{2} I_{fA2}$.

The steady state profiles of the reactor state variables (i.e., X_1: monomer conversion, X_2: initiator conversion, T: reactor temperature) are illustrated in Figure 4(a) for these three different initiator systems:

Monofunctional initiator (A1):

$k_d = 6.824 \times 10^{10} \exp(-22{,}800/RT)$, sec^{-1}

$I_{fA1} = 0.05$ mol/l

Monofunctional initiator (A2):

$k_d = 6.594 \times 10^{14} \exp(-30{,}500/RT)$, sec^{-1}

$I_{fA2} = 0.05$ mol/l

Bifunctional initiator (B):

$k_{d1} = 6.824 \times 10^{10} \exp(-22{,}800/RT)$, sec^{-1}

$k_{d2} = 6.594 \times 10^{14} \exp(-30{,}500/RT)$, sec^{-1}

$I_{fB} = 0.025$ mol/l

Note that the steady state profiles of X_1, X_2 and T for the bifunctional initiator (B) are approximately in the middle of those for the two monofunctional initiator systems. However, the molecular weight properties such as number average chain length (X_N) and polydispersity (X_W/X_N) for the bifunctional initiator system are quite different from those for the monofunctional initiator systems as shown in Figure 4(b). At high monomer conversions, the bifunctional initiator system produces polymers of significantly higher molecular weight than those obtained by the monofunctional initiators. The polydispersity is slightly higher for the bifunctional

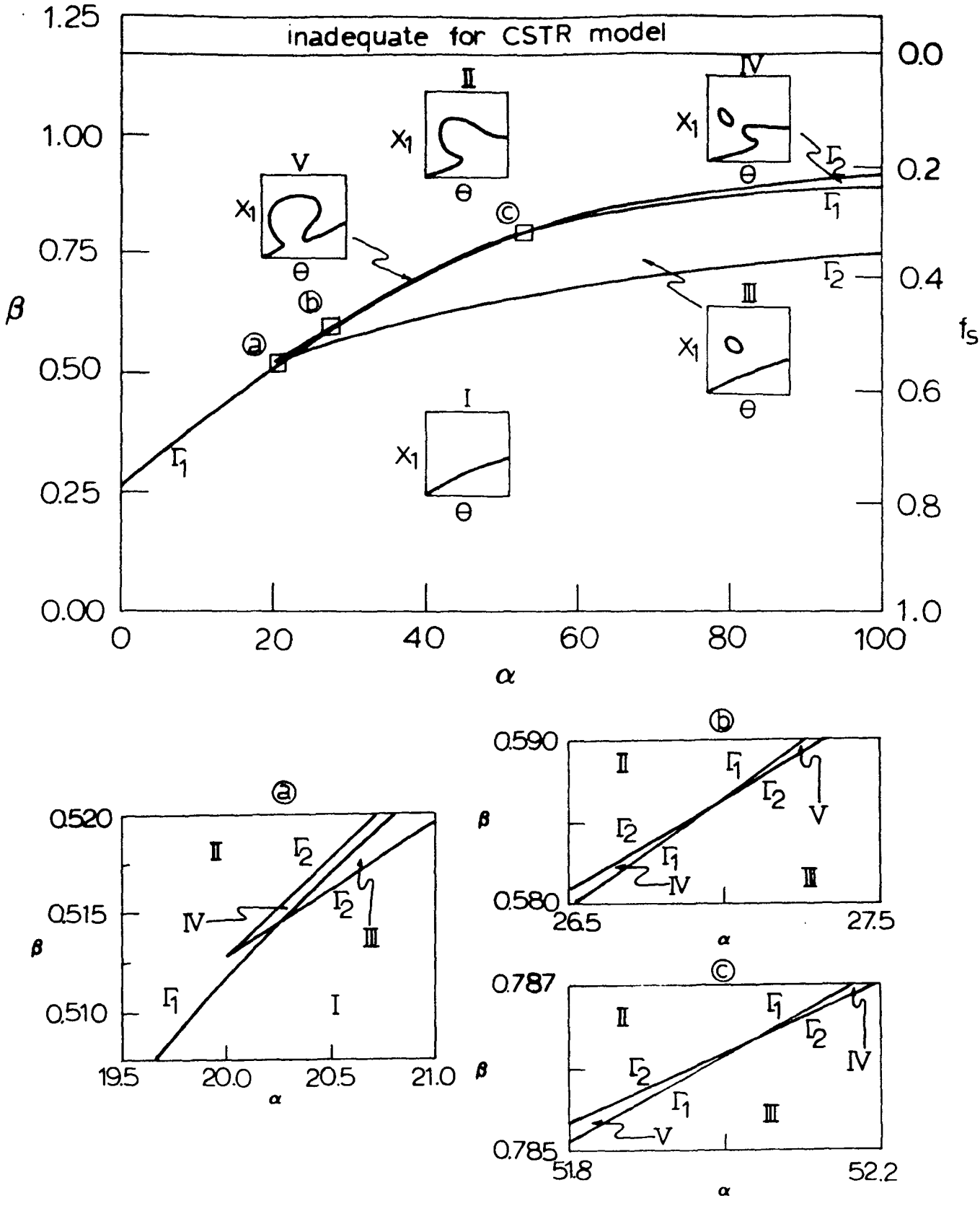

Figure 3(a) Steady state behavior regions for styrene polymerization in a CSTR with monofunctional initiator A1, δ=0.01, I_{fA1}=0.05 mol/l.

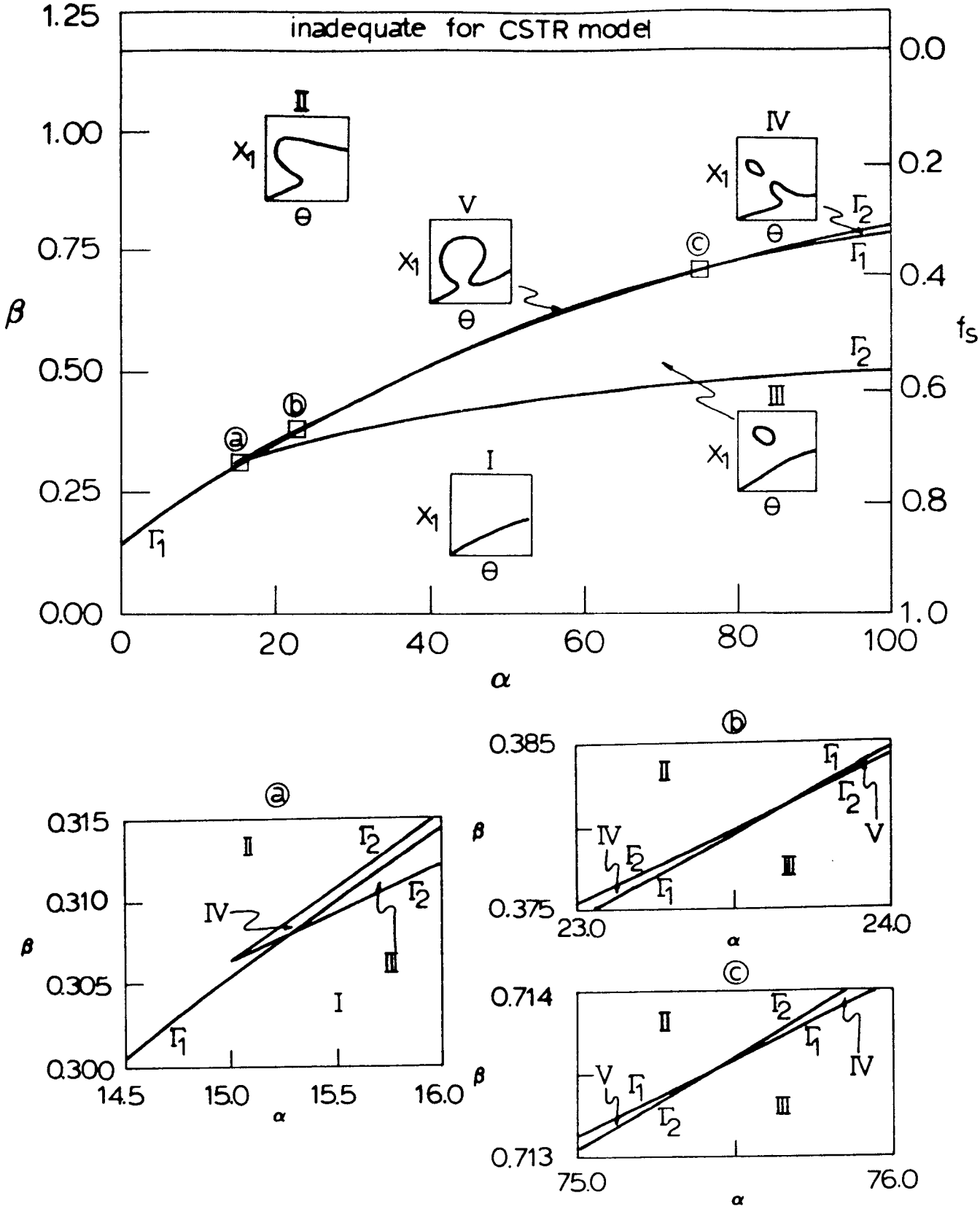

Figure 3(b) Steady state behavior regions for styrene polymerization in a CSTR with monofunctional initiator A2, δ=0.01, I_{fA2}=0.05 mol/l.

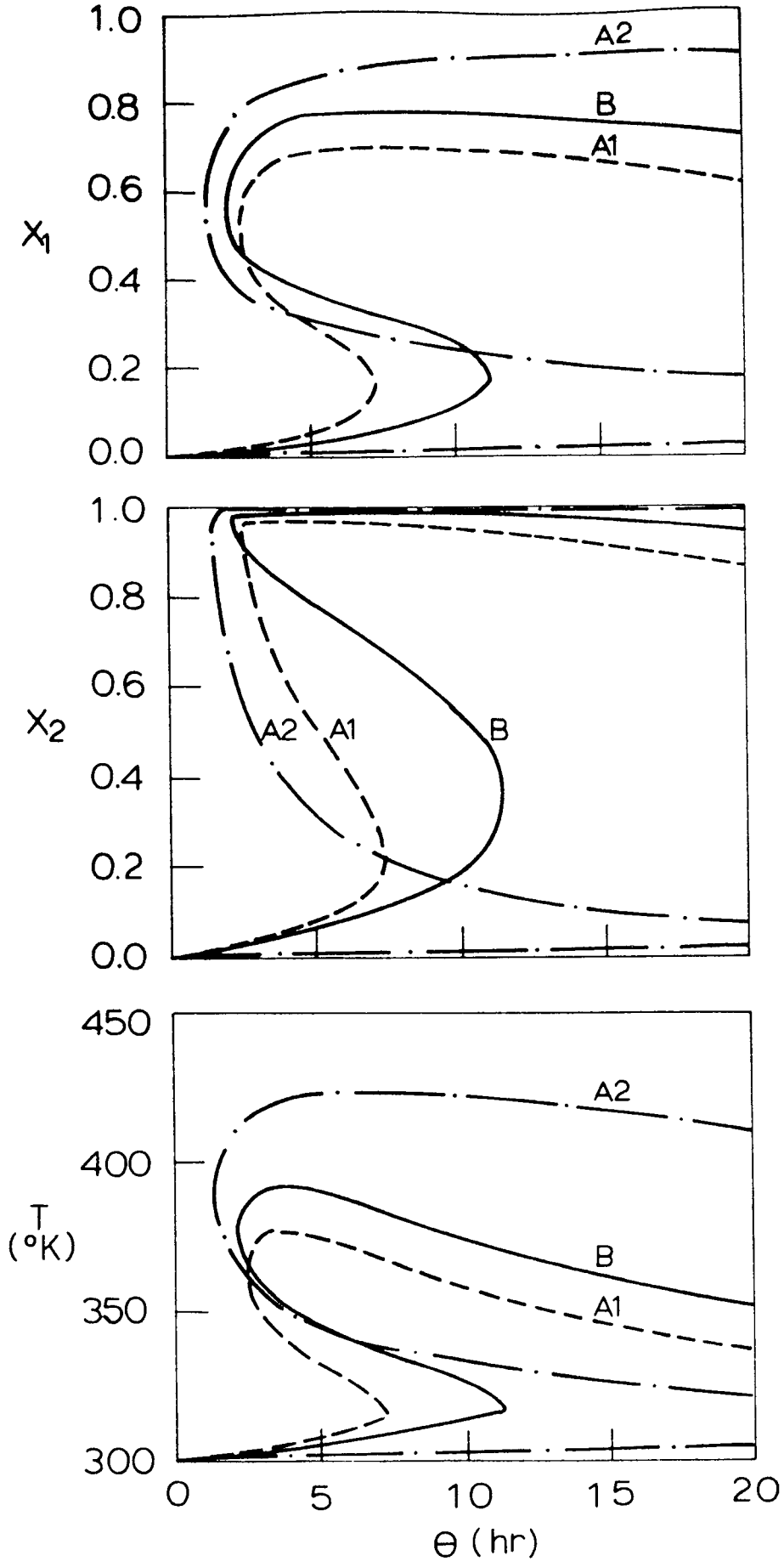

Figure 4(a) Steady state profiles of state variables for three initiator systems: α=15, β=0.5126, δ=0.01, I_{fB}=0.025 mol/l, I_{fA1}=I_{fA2}=0.05 mol/l.

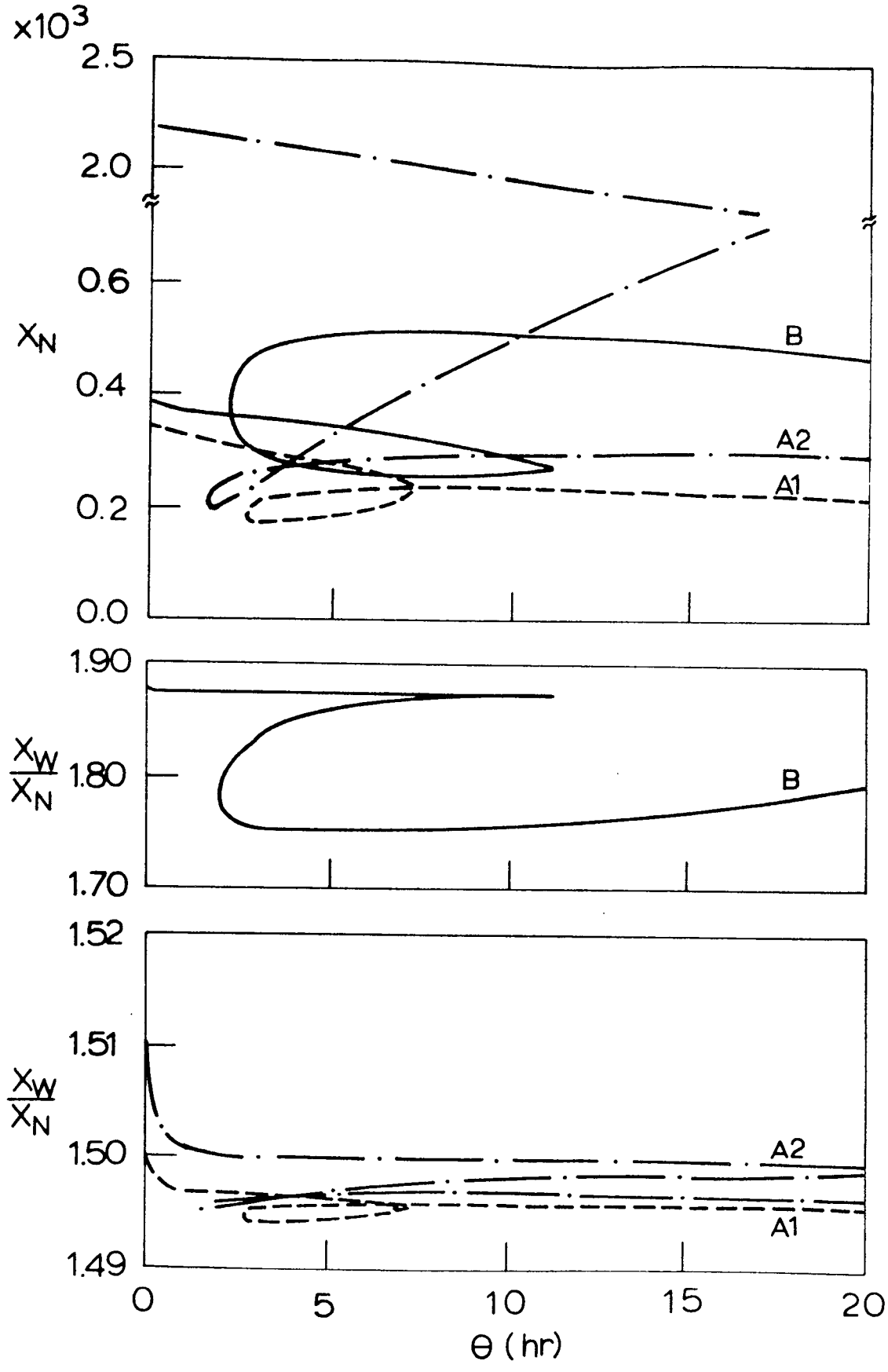

Figure 4(b) Steady state profiles of number average chain length and polydispersity: α=15, β=0.5126, δ=0.01, I_{fB}=0.025 mol/l, I_{fA1}=I_{fA2}=0.05 mol/l.

initiator system than for the monofunctional initiator systems due to the presence of various polymeric species of different chain lengths. The variations of X_N with steady state temperature and monomer conversion are more clearly illustrated in Figure 4(c). The highest conversion is obtainable by using the "slow" initiator (initiator A2) at high temperatures and long residence time; however, both high monomer conversion and high molecular weight of polymers are obtained by using the bifunctional initiator (B) at shorter residence time. The high molecular weight obtained by use of the bifunctional initiator is due to the extended lifetime of peroxide groups which reside in various polymeric species such as Q_n, T_n and Z_n.

Figure 4(d) illustrates the X_N of various inactive polymers and their weight fractions in the polymer. Note that as steady state reaction temperature increases (e.g. upper solution branch, Figure 4(a)), the decomposition of the peroxide groups in T_n and Z_n-type polymers is increased and more P_n or Q_n-type polymers are produced(cf. Eqs. (6) and (7)). When the growth of these live polymeric radicals is terminated, polymers of much higher molecular weight are obtained. It is also interesting to note in Figures 4(b) and 4(d) that when the concentrations of T_n and Z_n-type polymers are low, polydispersity is lowered due to the reduced heterogeneity of the polymer chain length distribution. The numerical calculation indicates that the concentrations of live polymers (P_n, Q_n and S_n) are order of magnitude lower than those of inactive polymers as shown in Figure 4(e). This means that the overall polymer molecular weight is determined predominantly by the dead or inactive polymers. Figure 4(d) also shows that Z_n-type polymer is a predominant species when the reactor is operated with residence time shorter than 12 hours. But the monomer conversion obtainable is only below 20% (Figure 4(a)).

The molar concentration (C_j) and the mole fraction (f_{mj}) of undecomposed peroxide groups in the primary initiator and various polymeric species are shown in Figure 4(f). In the middle steady state branch (i.e., $\theta = 2 \sim 12$ hours) where the monomer conversion is about 20~70%, the undecomposed peroxides reside mostly in T_n and Z_n-type polymers. However, as monomer conversion and reactor temperature increase (i.e., upper solution branch), the concentrations of peroxides in those inactive polymers decrease sharply by thermal decomposition and, as a result, the polymer molecular weight increases. If the production of polymers containing high

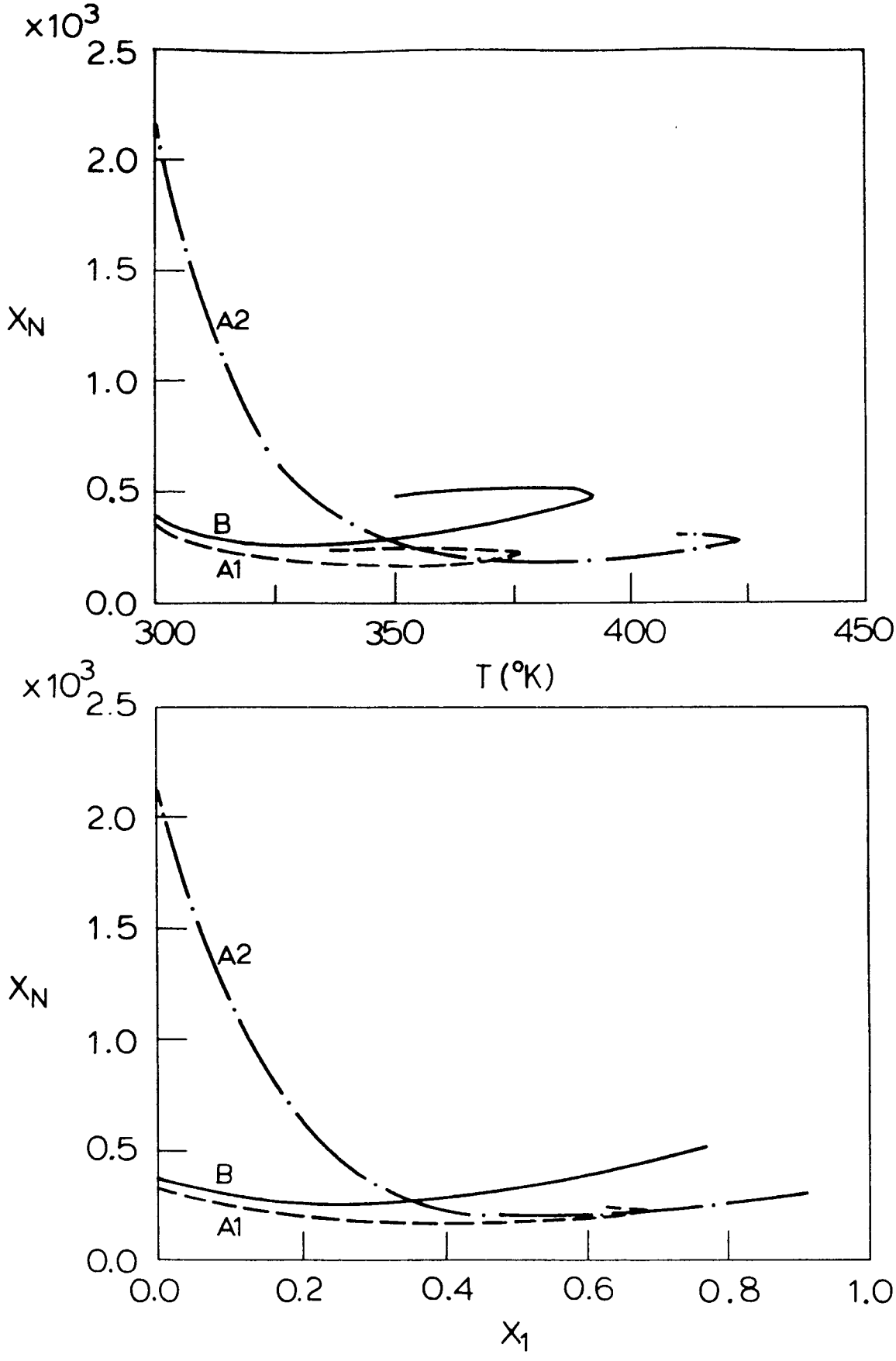

Figure 4(c) Steady state profiles of number average chain lengths vs. temperature and monomer conversion (X_1): α=15, β=0.5126, δ=0.01, I_{fB}=0.025 mol/l, I_{fA1}=I_{fA2}=0.05 mol/l.

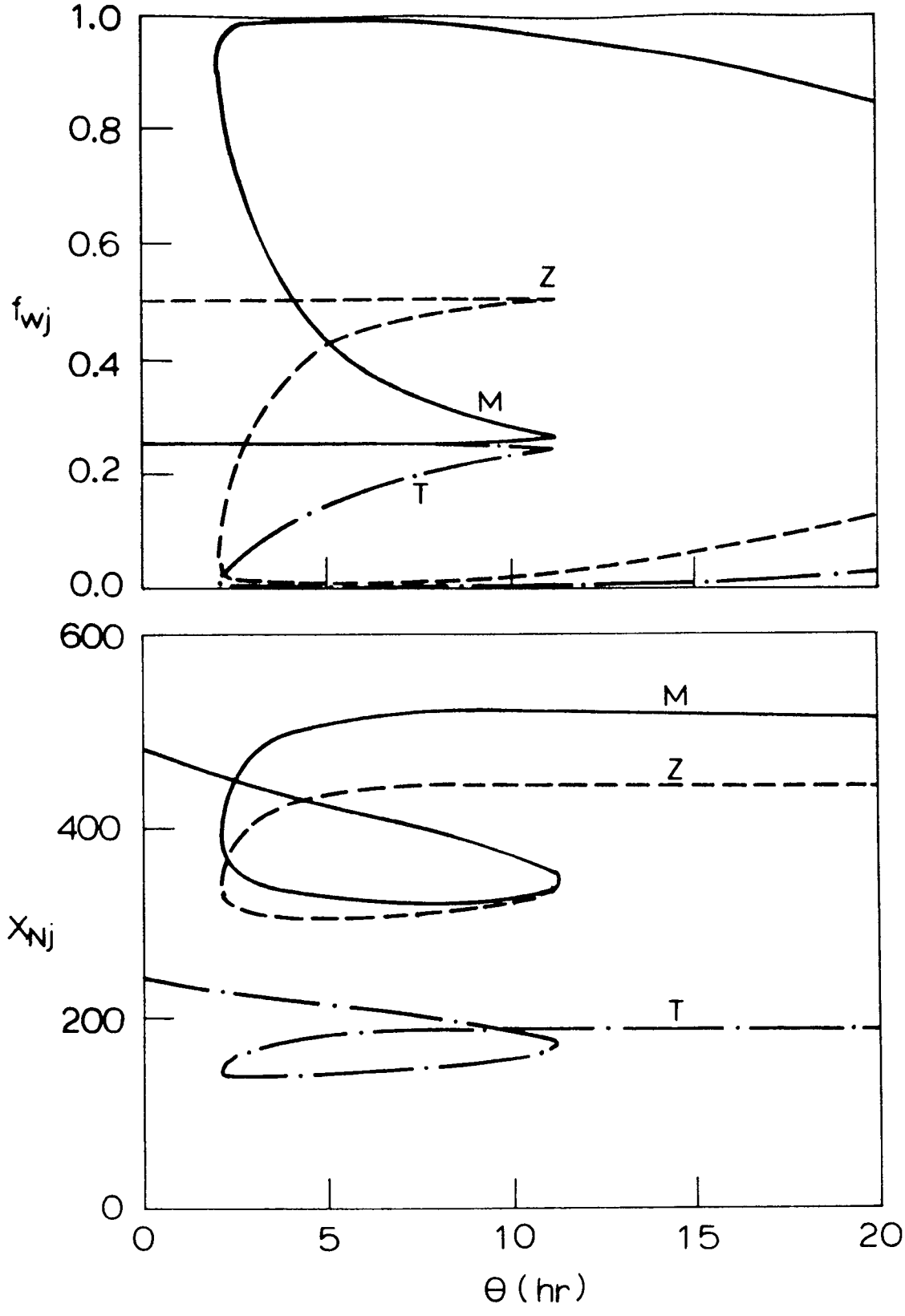

Figure 4(d) Weight fraction and number average chain length profiles of various inactive polymers: α=15, β=0.5126, δ=0.01, I_{fB}=0.025 mol/l.

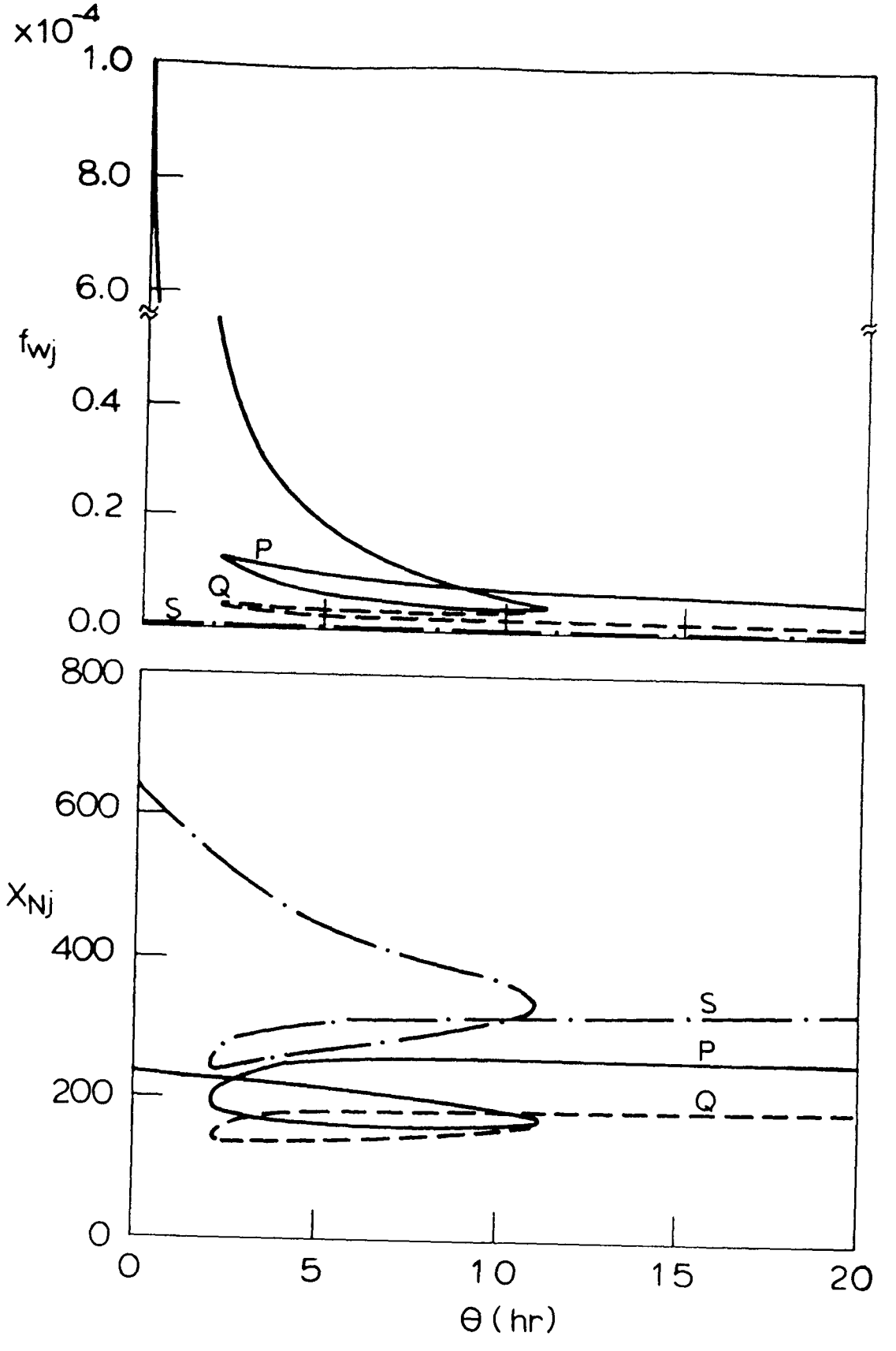

Figure 4(e) Weight fraction and number average chain length profiles of various live polymers: α=15, β=0.5126, δ=0.01, I_{fB}=0.025 mol/l.

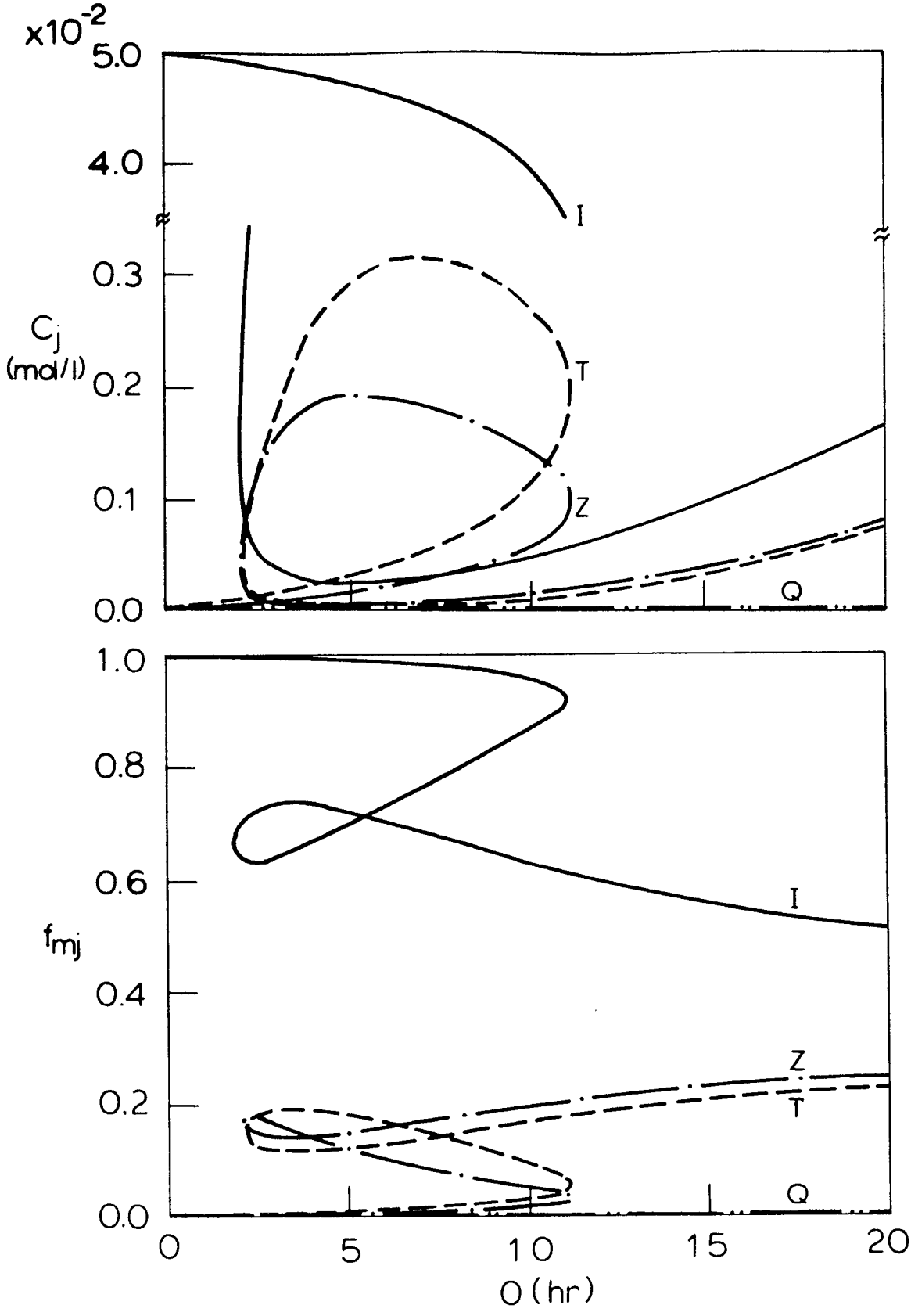

Figure 4(f) Distribution of undecomposed peroxides in various species: C_j= molar concentration of diperoxide in species j, f_{mj}= mole fraction of peroxides in species j, α=15, β=0.5126, δ=0.01, I_{fB}=0.025 mol/l.

concentration of peroxide is desired, the reactor should be operated at the middle steady state which may be open loop unstable. Such reactor conditions may be practically important, if free radical block copolymerization is performed in a series of CSTRs operating at different polymerization conditions in order to minimize the formation of homopolymers. A special stabilizing control is of course required to operate the reactor at such steady states.

The steady state reactor behavior for three different values of α (dimensionless heat transfer coefficient) with the bifunctional initiator is shown in Figures 5(a) and 5(b). As predicted in Figure 2, the S-shaped steady state curves become more exaggerated as α increases for fixed value of β and isola begins to appear with further increase in α. Figure 5(b) illustrates that polymer composition also changes significantly with variation in α. Note that the weight fractions of inactive polymers (T_n, Z_n-type) which contain undecomposed peroxide groups increase with α at long reactor residence time (e.g. $\theta > 10$ hrs.).

Concluding Remarks

In this paper, the steady state characteristics of styrene polymerization in a CSTR with bifunctional initiators have been investigated. For the diperoxyester initiator system considered in this study, six different polymeric species are identified according to their end groups. The polymeric species carrying undecomposed peroxides on chain ends can reinitiate the propagation and, as a result, overall lifetime of radicals is extended and the molecular weight of polymer can be significantly increased. It is also shown that five unique regions of steady state behavior of the polymerization reactor are present. Compared with monofunctional initiator systems, the bifunctional initiators provide higher monomer conversion and polymers of higher molecular weight. This implies that wide range of reactor operating conditions can be used to produce polymers of high molecular weight more effectively with bifunctional initiators. Our simulations also show that CSTRs can be used to produce reactive polymers containing undecomposed peroxide groups. Analysis of steady state stability and transient reactor behavior will be reported in our forthcoming paper.

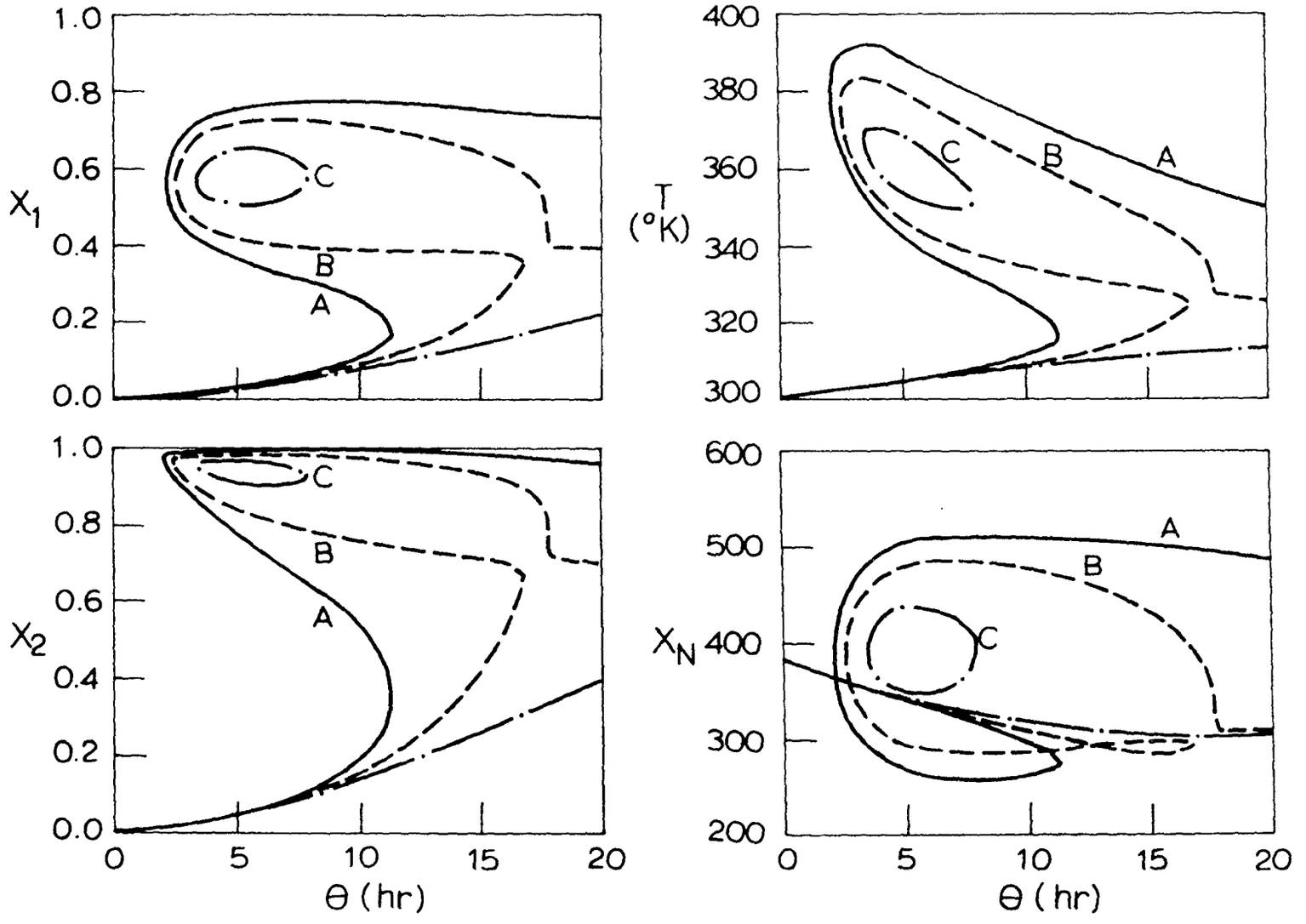

Figure 5(a) Steady state profiles of state variables for varing α values: β=0.5126, δ=0.01, I_{fB}=0.025 mol/l, α; A=15.0, B=18.3, C=22.0.

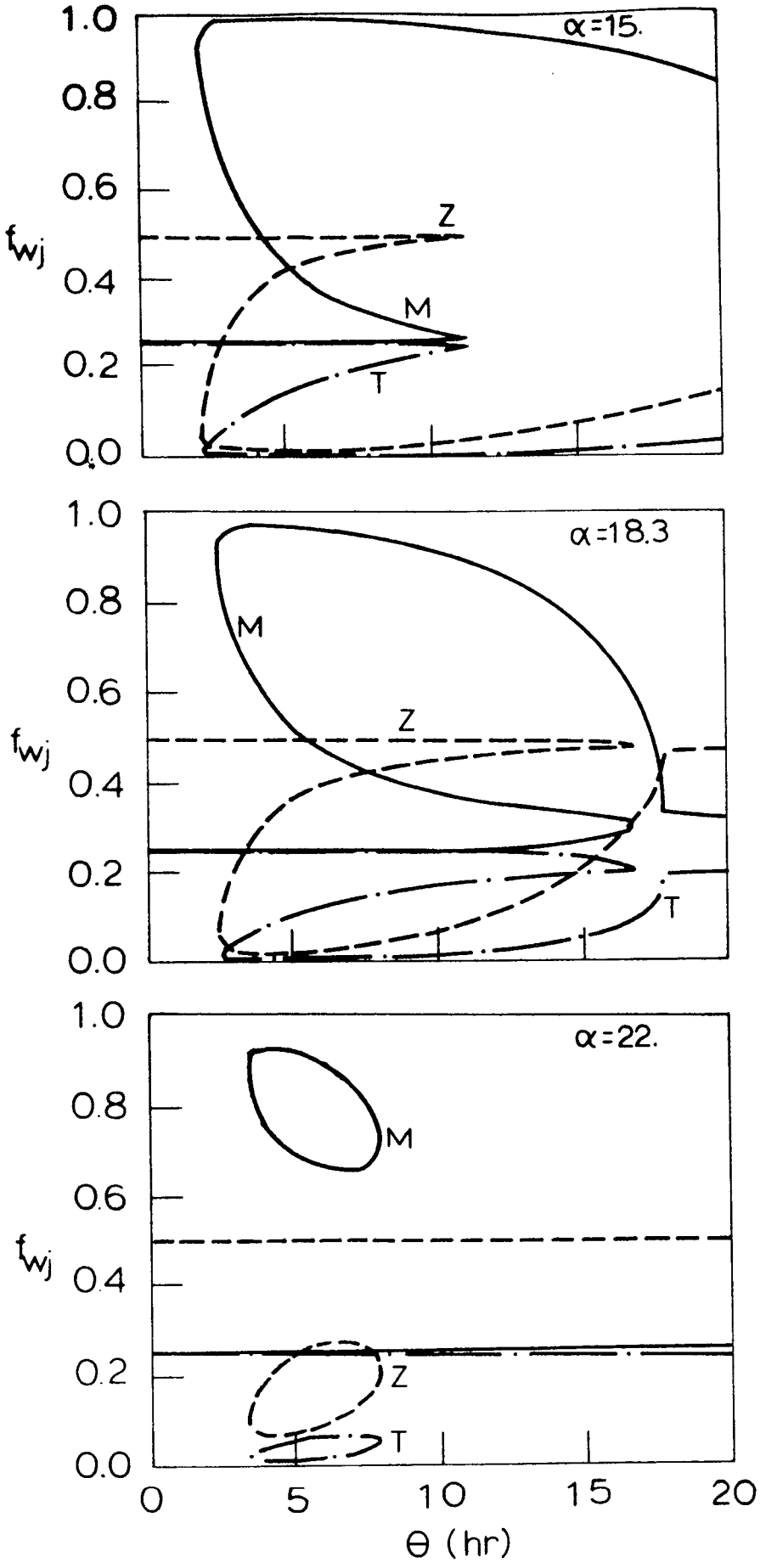

Figure 5(b) Weight fraction profiles of inactive polymers for varing α values: β=0.5126, δ=0.01, I_{fB}=0.025 mol/l.

Acknowledgement

This research was supported by the Systems Research Center at the University of Maryland through SRC Fellowship to Kim. Authors are also indebted to the Computer Science Center of the University of Maryland for computing time.

References

Balakotaiah, V., and D. Luss, "Analysis of the Multiplicity Patterns of a CSTR", *Chem. Eng. Commun.*, **13**, 112-132 (1981).

Brandrup, J., and E. H. Immergut (eds.), "*Polymer Handbook*", Second ed., Wiley, New York, 1975.

Choi, K. Y., and G. D. Lei, "Modeling of Free Radical Polymerization of Styrene by Bifunctional Initiators with Peroxide Groups of Unequal Thermal Stabilities", submitted to *AIChE J.* for publication (1986).

Friis, N., and A. E. Hamielec, "Gel Effect in Emulsion Polymerization of Vinyl Monomers", *ACS Symp. Ser.*, **24**, 82-91 (1976).

Gunesin, B. Z., and I. Piirma, "Block Copolymers Obtained by Free Radical Mechanism. II. Butyl Acrylate and Methyl Methacrylate", *J. Appl. Poly. Sci.*, **26**, 3103-3115 (1981).

Hamer, J. W., T. A. Akramov and W. H. Ray, "The Dynamic Behavior of Continuous Polymerization Reactors-II", *Chem. Eng. Sci.*, **36**, 1897-1914 (1981).

Ivanchev, S. S., "New Views on Initiation of Radical Polymerization in Homogeneous and Heterogeneous Systems. Review", *Poly. Sci. USSR*, **20**, 2157-2181 (1979).

Kim, K. J., Ph. D. Thesis, University of Maryland (1989, *expected*).

O'Driscoll, K. F., and J. C. Bevington, "The Effect of Multifunctinal Initiators on Molecular Weight in Free Radical Polymerization", *Eur. Poly. J.*, **21**(12), 1039-1043 (1985).

Piirma, I., and L. P. H. Chou, "Block Coploymers Obtained by Free Radical Mechanism. I. Methyl Methacrylate and Styrene", *J. Appl. Poly. Sci.*, **24**, 2051-2070 (1979).

Prisyazhnyuk, A. I., and S. S. Ivanchev, "Diperoxides with Differing Thermal Stabilities of the Peroxide Groups as Initiators of Radical Polymerization and Block Copolymerization", *Poly. Sci. USSR*, **12**(2), 514-524 (1970).

Schmidt, A. D., A. B. Clinch and W. H. Ray, "The Dynamic Behavior of Continuous Polymerization Reactors-III. An Experimental Study of Multiple Steady States in Solution Polymerization", *Chem. Eng. Sci.*, **39**(3), 419-432 (1984).

Waltz, R., and W. Heitz, "Preparation of $(AB)_n$-type Block Copolymers by Use of Polyazoesters", *J. Poly. Sic.:Poly. Chem. Ed.*, **16**, 1807-1814 (1978).

Nomenclature

A_c	heat transfer area (cm^2)
C_p	heat capacity of reaction mixture (cal/mol°K)
Da	Damkohler number (-)
E_d	decomposition activation energy (cal/mol)
E_p	activation energy of propagation (cal/mol)
f_s	solvent volume fraction (-)
g_t	gel effect correlation factor, k_t/k_{to} (-)
h_c	heat transfer coefficient ($cal/cm^2sec°K$)
ΔH_r	heat of reaction (cal/mol)
I	initiator concentration (mol/l)
I_f	initiator concentration in feed (mol/l)
I_{fB}	feed concentration of bifunctional initiator (mol/l)
I_{fA1}	feed concentration of monofunctional initiator A1 (mol/l)
I_{fA2}	feed concentration of monofunctional initiator A2 (mol/l)
k_d	initiator decomposition rate constant (sec^{-1})
k_i	initiation rate constant (l/mol.sec)
k_p	propagation rate constant (l/mol.sec)
k_t	combination termination rate constant (l/mol.sec)
k_{to}	combination termination rate constant at zero conversion (l/mol.sec)
M	monomer concentration (mol/l)
M_f	feed monomer concentration (mol/l)
M_n	dead polymer concentration of n monomer units (mol/l)
P_n	live polymer concentration of n monomer units (mol/l)
PD	polydispersity (-)
Q_n	concentration of live polymer species defined in Table 1 (mol/l)
q	volumetric feed flow rate (l/sec)
R	primary radical concentration (mol/l)
R'	concentration of primary radicals containing undecomposed peroxide group (mol/l)
S_n	concentration of live polymer species defined in Table 1 (mol/l)
T	temperature (°K)
T_c	coolant temperature (°K)
T_f	feed temperature (°K)
T_n	concentration of inactive polymer species defined in Tabile 1 (mol/l)

t dimensionless time (-)

t' time (sec)

V reactor volumer (cm^3)

X_1 monomer conversion (-)

X_2 initiator conversion (-)

X_3 dimensionless temperature (-)

X_p dimensionless total live polymer concentration (-)

X_N number average polymer chain length (-)

X_W weight average polymer chain length (-)

Z_n concentration of inactive polymer species defined in Table 1 (mol/l)

Greek Letters

α dimensionless heat transfer coefficient (-)

β dimensionless heat of reaction (-)

γ dimensionless propagation activatin energy(-)

γ_1 dimensionless decomposition activatin energy (-)

δ dimensionless coolant temperature (-)

ρ density of reaction mixture (mol/l)

$\lambda_{\xi,k}$ k-th moment of polymer species ξ (-)

λ_k^d k-th moment of dead polymer (-)

Figure Captions

Figure 1 Gel effect correlations for styrene polymerization

Figure 2 Steady state behavior regions for styrene polymerization in a CSTR with bifunctinal initiator, δ=0.01, I_{fB}=0.025 mol/l.

Figure 3(a) Steady state behavior regions for styrene polymerization in a CSTR with monofunctional initiator A1, δ=0.01, I_{fA1}=0.05 mol/l.

Figure 3(b) Steady state behavior regions for styrene polymerization in a CSTR with monofunctional initiator A2, δ=0.01, I_{fA2}=0.05 mol/l.

Figure 4(a) Steady state profiles of state variables for three initiator systems: α=15, β=0.5126, δ=0.01, I_{fB}=0.025 mol/l, I_{fA1}=I_{fA2}=0.05 mol/l.

Figure 4(b) Steady state profiles of number average chain length and polydispersity: α=15, β=0.5126, δ=0.01, I_{fB}=0.025 mol/l, I_{fA1}=I_{fA2}=0.05 mol/l.

Figure 4(c) Steady state profiles of number average chain lengths vs. temperature and monomer conversion (X_1): α=15, β=0.5126, δ=0.01, I_{fB}=0.025 mol/l, I_{fA1}=I_{fA2}=0.05 mol/l.

Figure 4(d) Weight fraction and number average chain length profiles of various inactive polymers: α=15, β=0.5126, δ=0.01, I_{fB}=0.025 mol/l.

Figure 4(e) Weight fraction and number average chain length profiles of various live polymers: α=15, β=0.5126, δ=0.01, I_{fB}=0.025 mol/l.

Figure 4(f) Distribution of undecomposed peroxides in various species: C_j= molar concentration of diperoxide in species j, f_{mj}= mole fraction of peroxides in species j, α=15, β=0.5126, δ=0.01, I_{fB}=0.025 mol/l.

Figure 5(a) Steady state profiles of state variables for varing α values: β=0.5126, δ=0.01, I_{fB}=0.025 mol/l, α; A=15.0, B=18.3, C=22.0.

Figure 5(b) Weight fraction profiles of inactive polymers for varing α values: β=0.5126, δ=0.01, I_{fB}=0.025 mol/l.

Appendix: Steady State Polymer Moments

Inactive Polymers

Zeroth moment :

$$\lambda_0^d = \frac{1}{2}\theta k_t P^2 \tag{A.1}$$

$$\lambda_{Z,0} = \frac{\theta k_t PQ}{1+\theta k_{d2}} \tag{A.2}$$

$$\lambda_{T,0} = \frac{\theta k_t Q^2}{2(1+\theta k_{d2})} \tag{A.3}$$

First moments :

$$\lambda_1^d = \theta k_t P \lambda_{P,1} \tag{A.4}$$

$$\lambda_{Z,1} = \frac{\theta k_t (P\lambda_{Q,1} + Q\lambda_{P,1})}{1+\theta k_{d2}} \tag{A.5}$$

$$\lambda_{T,1} = \frac{\theta k_t Q \lambda_{Q,1}}{1+\theta k_{d2}} \tag{A.6}$$

Second moment :

$$\lambda_2^d = \theta k_t (P\lambda_{P,2} + \lambda_{P,1}^2) \tag{A.7}$$

$$\lambda_{Z,2} = \frac{\theta k_t (2\lambda_{P,1}\lambda_{Q,1} + P\lambda_{Q,2} + Q\lambda_{P,2})}{1+\theta k_{d2}} \tag{A.8}$$

$$\lambda_{T,2} = \frac{\theta k_t (\lambda_{Q,1}^2 + Q\lambda_{Q,2})}{1+\theta k_{d2}} \tag{A.9}$$

Live Polymers

First moments:

$$\lambda_{P,1} = -\frac{(a_1 + b_1\lambda_{Q,1})}{c_1} \tag{A.10}$$

$$\lambda_{Q,1} = -\frac{d_1}{e_1} \tag{A.11}$$

$$\lambda_{S,1} = \frac{k_p M_f (1 - X_1) S + k_{d2}\lambda_{Q,1}}{k_t (P + Q)} \tag{A.12}$$

Second moments:

$$\lambda_{P,2} = -\frac{(a_2 + b_2\lambda_{Q,2})}{c_2} \tag{A.13}$$

$$\lambda_{Q,2} = -\frac{d_2}{e_2} \tag{A.14}$$

$$\lambda_{S,2} = \frac{k_p M_f (1 - X_1)(2\lambda_{S,1} + S) + k_t \lambda_{S,1}^2 + \lambda_{Q,2}}{k_t (P + Q)} \tag{A.15}$$

where

$$a_1 = f_i k_{d1} I_f (1 - X_2) + k_p M_f (1 - X_1) P + \frac{k_p M_f (1 - X_1) S P}{P + Q} + k_{d2}(Q + T + Z) \tag{A.16}$$

$$b_1 = \frac{k_{d2} P}{P + Q} + \frac{\theta k_t k_{d2} P}{1 + \theta k_{d2}} \tag{A.17}$$

$$c_1 = \frac{\theta k_t k_{d2} Q}{1 + \theta k_{d2}} - k_t (P + Q) \tag{A.18}$$

$$d_1 = f_i k_{d1} I_f (1 - X_2) + k_p M_f (1 - X_1) Q + \frac{k_p M_f (1 - X_1) SQ}{P + Q} \quad (A.19)$$

$$e_1 = \frac{k_{d2} Q}{P + Q} - k_t (P + Q) + \frac{\theta k_t k_{d2} Q}{1 + \theta k_{d2}} - k_{d2} \quad (A.20)$$

$$\begin{aligned} a_2 = {} & f_i k_{d1} I_f (1 - X_2) + k_p M_f (1 - X_1)(2\lambda_{P,1} + P) \\ & + k_{d2}(Q + T + Z) + 2k_t \lambda_{P,1} \lambda_{S,1} \\ & + \frac{2\theta k_t k_{d2} \lambda_{P,1} \lambda_{Q,1}}{1 + \theta k_{d2}} \\ & + \frac{k_p M_f (1 - X_1) P (2\lambda_{S,1} + S) + k_t P \lambda_{S,1}^2}{P + Q} \end{aligned} \quad (A.21)$$

$$b_2 = \frac{k_{d2} P}{P + Q} + \frac{\theta k_t k_{d2} P}{1 + \theta k_{d2}} \quad (A.22)$$

$$c_2 = \frac{\theta k_t k_{d2} Q}{1 + \theta k_{d2}} - k_t (P + Q) \quad (A.23)$$

$$\begin{aligned} d_2 = {} & f_i k_{d1} I_f (1 - X_2) + k_p M_f (1 - X_1)(2\lambda_{Q,1} + Q) \\ & + \frac{\theta k_t k_{d2} \lambda_{Q,1}^2}{1 + \theta k_{d2}} + 2k_t \lambda_{Q,1} \lambda_{S,1} \\ & + \frac{k_p M_f (1 - X_1)(2\lambda_{S,1} + S) Q + k_t Q \lambda_{S,1}^2}{P + Q} \end{aligned} \quad (A.24)$$

$$e_2 = \frac{\theta k_t k_{d2} Q}{1 + \theta k_{d2}} - k_{d2} - k_t (P + Q) + \frac{k_{d2} Q}{P + Q} \quad (A.25)$$